Hindawi
Complexity
Volume 2018, Article ID 8261549, 11 pages
https://doi.org/10.1155/2018/8261549

Research Article

Sensor Fault Diagnosis Based on Fuzzy Neural Petri Net

Jiming Li, Xiaolin Zhu, and Xuezhen Cheng

College of Electrical Engineering and Automation, Shandong University of Science and Technology, 579 Qianwangang Road, Huangdao District, Qingdao, Shandong Province 266590, China

Correspondence should be addressed to Xuezhen Cheng; zhenxc6411@163.com

Received 8 May 2018; Revised 19 September 2018; Accepted 9 October 2018; Published 23 October 2018

Guest Editor: Zhile Yang

This study aims to improve the operating stability of the resistance strain weighing sensor and eliminate fuzzy factors in fault diagnosis. Based on fuzzy techniques for fault diagnosis, the proposed fuzzy Petri net model uses the fault logical relationship between a sensor and an improved Petri net model. A formula for confidence-based reasoning is proposed using an algorithm, which combines neural network regulation algorithm with a transition-enabled ignition judgment matrix. This formula can yield an accurate assessment of the operating state of the sensor. Backward inference and the minimum cut set theory are also combined to obtain the priority of faults, which helps avoid blind and ambiguous maintenance. The sensor model was analyzed, and its accuracy and validity were verified through statistical analysis and comparison with other methods of fault diagnosis.

1. Introduction

The resistance strain weighing sensor (hereinafter referred to as "the sensor") is a core component of electronic weighing instruments, and its quality directly influences the accuracy of measurement. In practical applications, due to the influence of raw materials, manufacturing processes, installation methods, service conditions, and the external environment, electronic weighing instruments are prone to various faults with uncertainty. Therefore, accurately predicting and diagnosing faults in these instruments are significant to ensure their accuracy and stability.

As an effective method of parallel computing and behavioral analysis [1], the Petri net has a rigorous mathematical formulation as well as a straightforward graphic description. In [2–5], fuzzy technology (a new technology based on fuzzy mathematics) was combined with the Petri net to propose the fuzzy Petri net (FPN) method of modeling, which has exhibited powerful parallel processing capability. However, optimizing the model structure and developing the matrix implementation remain to be further researched. It is important to find a model that is representative of real environments.

For calculations in FPN, although the problem in the FPN related to matrix reasoning was solved in [1, 6], its weight and other parameters remain undetermined, and accurate data are needed to ensure the correctness of the diagnosis.

Based on the operator's diagnostic experience, a method for fault diagnosis in expert systems (ES) can be used as the operating logic of the protection relay and circuit breakers and has been applied to power systems. Methods of fault analysis based on ES have been reported in the literature [7–9]. For example, an advanced logic-based ES was applied in [7]. The General Diagnosis Engine was used to analyze place information and evaluate security [9]. However, ES-based methods of analysis have shortcomings, such as requiring complex knowledge acquisition and maintenance and slow reasoning. Modeling based on directivity was proposed in [10] to reduce the dimensionality of the incidence matrix and simplify the calculation model, but it fails to provide a sufficient description of weight. The method proposed in [11] significantly improves the fault tolerance of the Petri net, but the Petri net model based on a time sequence does not apply to a static Petri net with adjustable weights.

Owing to fuzzy behavior in the FPN, a number of methods for data determination have been proposed. The BP (back propagation) algorithm endows the Petri net with the capability of self-learning [12–14], resulting in clear weight values. However, the model does not improve accordingly.

The BP neural network has been combined with the traditional fuzzy fault Petri net to develop the adaptive FPN [15, 16], which improves the capability of the traditional fuzzy fault Petri net to learn weights. However, it fails to explicitly show how to determine the transition confidence coefficient, leaving the system with a large number of uncertainties. The forward-backward algorithm was used to implement reasoning pertaining to unobservable place events in the model [17]. Many other fault diagnosis methods, such as data fusion and the support vector machine (SVM), were proposed as well. Reference [18] has been applied to effectively solve such problems as nonlinearity and high dimensionality. However, due to the characteristics of the SVM, multiple dichotomies are currently used to solve multiclassification problems; in this context, the excessive classification is associated with unnecessary complexity of calculation, and hence a faster method is needed to ensure system stability.

This study proposes a method to diagnose sensor faults based on fuzzy neural Petri net. With the resistance strain weighing sensor as the research object, its FPN fault model is created. The neural network is applied to adjust the weight, with the abandonment of the transition confidence coefficient. The MYCIN confidence reasoning algorithm is optimized based on the sigmoid function and, consequently, fault diagnosis is accomplished based on the minimum cut set of fault rate.

2. Improved Fuzzy Fault Petri Net

2.1. Structure of the Fuzzy Fault Petri Net. Based on the Petri net and fuzzy Petri net theory [19–22], a nine-parameter model is defined as $S_P = (P, T, I, O, K, W, \alpha, f, \lambda)$.

The variables are as follows:

(1) $P = (p_1, p_2, \ldots, p_n)^T$ is a set of place faults, including all faults relating to the sensor, such as "broken gate of the output-adjusting resistance," "overloaded weighing," and "excessively large sensitivity of diaphragm shunting."

(2) $T = (t_1, t_2, \ldots, t_n)^T$ is a set of transitions. If a transition is enabled, $t_j = 1$; otherwise, $t_j = 0$.

(3) I is the input matrix of the Petri net.

(4) O is the output matrix of the Petri net.

(5) $K = (k_1, k_2, \ldots, k_n)^T$ denotes the place label vector. When a fault occurs in place i, $k_j = 1$; otherwise, $k_j = 0$.

(6) $W = \{\omega_{ij}\}$ is an $n \times m$ matrix of the weight of the place. When $\forall t \in T, P_k \in I(t), \sum_{j=1}^{n} \omega_k = 1$.

(7) $\alpha = (\alpha_1, \alpha_1, \ldots, \alpha_n)^T$ is an n-dimensional vector of the confidence coefficients of the place, denoting the confidence of occurrence of a fault event.

(8) $f = (f_1, f_1, \ldots, f_n)^T$ is a set of probabilities of the fuzzy occurrence of place events, where f_j denotes the probability of occurrence of place event p_i.

(9) $\lambda = (\lambda_1, \lambda_1, \ldots, \lambda_n)^T$ is the threshold vector of transition.

2.2. Structure of the Improved Fuzzy Fault Petri Net. The connection of sensor components is tight, multiple mappings between faults, with the complex and diverse fault propagation mode. Based on this, firstly, the structure of the sensor is analyzed, according to the fuzzy relation to obtain the fault logic relationship, and then the FPN mode is established following the basic rules of Petri net, where the confidence reasoning algorithm is optimized based on the sigmoid function. In other words, based on the original fuzzy Petri net, the sigmoid function replaces the initial transition confidence μ to describe the rules to deduce the FPN model and the expression of fuzzy information. The confidence values of fault events occurring in different places can be obtained through reasoning, which provides the necessary conditions for the positive and negative instances of reasoning pertaining to faults. Figure 1 shows the basic elements of the improved Petri net.

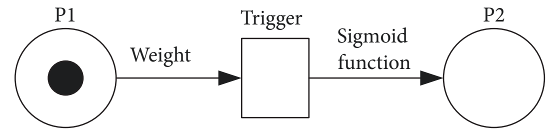

Figure 1: Improved Petri net model.

3. Algorithms for FPN Fault Reasoning

To clearly and concisely present the reasoning and calculation of each matrix during the reasoning for the FPN model, the Petri net is used to describe the capability of the concurrency system and the mathematical theory of the FPN to define five special operators [23]:

(1) The comparison operator $\diamond$: $C = A \diamond B$, where A, B, and C are $m \times n$ matrices. When $a_{ij} > b_{ij}, c_{ij} = 1$; when $a_{ij} < b_{ij}$, $c_{ij} = 0, i = 1, 2, \ldots, m; j = 1, 2, \ldots, n$.

(2) The minimum operator $\wedge$: $C = A \wedge B$, where A, B, and C are $m \times n$ matrices; $c_{ij} = \min(a_{ij}, b_{ij})$, where $i = 1, 2, \ldots, m$; $j = 1, 2, \ldots, n$.

(3) The maximum operator $\vee$: $C = A \vee B$, where A, B, and C are $m \times n$ matrices; $c_{ij} = \max(a_{ij}, b_{ij})$, where $i = 1, 2, \ldots, m$; $j = 1, 2, \ldots, n$.

(4) The direct product operator $*$: $C = A * B$, where A, B, and C are $m \times n$ matrices; b is an n-dimensional vector; $c_{ij} = a_{ij} * b_i$, where $i = 1, 2, \ldots, m$; $j = 1, 2, \ldots, n$.

(5) The multiplication operator $\otimes$: $C = A \otimes B$, where A, B, and C are $m \times q$, $q \times n$, and $m \times n$ matrices, respectively; $c_{ij} = \max_{i \le k \le q}(a_{ij}, b_{ij})$, where $i = 1, 2, \ldots, m$; $j = 1, 2, \ldots, n$.

3.1. Confidence Algorithm. The confidence algorithm is modified to achieve higher computational efficiency. Following the reasoning calculation, the confidence values of all places are obtained and function as the basis of fault evaluation and diagnosis.

Weight matrix $W = \{\omega_{ij}\}$, where $\omega_{ij} \in (0, 1)$. When there is a directional arc p_i to t_j, ω_{ij} is the weight from p_i to t_j. When there is a directional arc t_j to p_i, $\omega_{ij} = 0$.

The reasoning formula is

$$\alpha^{k+1} = \alpha^k \vee \left[1 + \exp\left(\rho^k\right)\right]^{-1} \tag{1}$$

where $\rho^k = O \bullet (W^T \cdot \alpha^k)$, $a_{i+1} = \alpha_i$; when and only when the reasoning is concluded; otherwise, it is continued.

3.2. Forward Reasoning. The forward reasoning based on the FPN model reflects the characteristics of fault propagation and predicts faults according to the work environment, the detection of components, or symptom-related information obtained by professionals. The faults that may occur are evaluated through the judgment matrix of transition firing and the flow of fault-state marking, and the corresponding response measures are then taken.

3.2.1. Transition Judgment

Definition 1. $\forall P_{Ij} \in I(t)$, $\sum_{j=1}^{n} \alpha(P_{Ij}) \bullet \omega_{Ij} \geq \lambda_t$, where t is enabled by potential transition.

Definition 2. If transition T can trigger ignition, there is a new confidence coefficient in the output place P_{Oj}; if not, the output place is 0.

$$\alpha\left(P_{Oj}\right) = \begin{cases} \left(\exp\left(\sum_j \alpha\left(P_{Ij} \bullet \omega_j\right)\right) + 1\right)^{-1}, & \sum_j \alpha\left(P_{Ij}\right) \bullet \omega_{Ij} \geq \lambda(t), \\ 0, & \sum_j \alpha\left(P_{Ij}\right) \bullet \omega_{Ij} < \lambda(t), \end{cases} \quad (2)$$

The transition-triggering ignition matrix is Y, where $Y = (y_1, y_2, \ldots, y_n)^T$.

$$Y = \left(W^T \bullet \alpha\right) \diamond \lambda \quad (3)$$

If the ignition conditions are met, $y_i = 1$; otherwise, $y_i = 0$. According to the rules of ignition, the transition-enabled ignition matrix reasoning corresponding to the token containing the place is calculated out based on [1]

$$\begin{aligned} Y_i &= y \wedge \left[\left(I * K_{i-1}\right)^T \bullet l_m\right], \quad i = 1, \\ Y_i &= y \wedge \left[I * \left(K_{i-1} - K_{i-2}\right)\right]^T \cdot l_m, \quad i = 2, 3, \ldots, \end{aligned} \quad (4)$$

where K_{i-1}, K_{i-2} denote the label vector of the i-1th ignition and $l_m = (1, 1, \ldots, 1)^T$ is an m-dimensional vector.

3.2.2. Reasoning Matrix of Fault-State Label Vector

$$K_i = K_{i-1} \oplus \left(A \otimes Y_i\right) \quad (5)$$

where A is the incidence matrix, $A = [a_{ij}] \in R^{n \times m}$, n is the number of places, and m is the number of transitions [10].

3.3. Backward Reasoning. FPN backward reasoning deduces the cause of a fault if it occurs. To avoid blind maintenance and improve the efficiency of tracking the source of the fault, the minimum cut set is introduced as the basis of fault derivation and diagnosis.

Definition 3. If the minimum cut set $G = \{p_1, p_2, \ldots, p_n\}$, the rate of fault occurrence is

$$f(G) = \frac{\left(\alpha_1 + \alpha_2 + \ldots + \alpha_n\right)}{n}, \quad n > 0 \quad (6)$$

The input and output places of FPN backward reasoning are the output and input places of FPN forward reasoning, respectively; namely, $I^- = O, O^- = I$.

The backward reasoning matrix is given by

$$\begin{aligned} Y^- &= \left[\left(I^- \triangle K_{i-1}^-\right) \otimes l_m\right] \wedge y, \\ K_i^- &= K_{i-1}^- \oplus \left(O^- \otimes Y_i^-\right), \\ & \qquad i = 1, 2, 3, \ldots, \end{aligned} \quad (7)$$

where Y_k^- is the backward-enabled transition sequence of the kth backward ignition.

4. Fault Analysis of the Resistance Strain Weighing Sensor

4.1. Determination of FPN Data. In reasoning relating to the fuzzy Petri net, the confidence coefficient of the initial place (the bottom place of FPN model) needs to be entered externally, whereas those of the middle place and the concluding places are generally obtained by the reasoning. Thus, the determination of the confidence coefficient (fuzzy token) pertaining to place mainly refers to the initial place. In this study, the method proposed in [24] is used to combine historical data with expert opinion to set the confidence coefficient of the initial place.

In the fuzzy Petri net, weight ω represents the degree to which each condition influences the conclusion and is mainly determined based on past studies. This is significantly subjective and uncertain. As the improved fuzzy Petri net possesses certain characteristics of a neural network, the neural network algorithm can be used to train, learn, and adjust the network. The adjustment algorithm is as follows:

d_i is the due output (expected output) of the ith element and y_i is its actual output. The element's error signal is given by

$$e_i = d_i - y_i \quad (8)$$

$$\mathrm{y_i} = \mathrm{v_i} \bullet \left(\sum \alpha_\mathrm{i} \bullet \omega_\mathrm{i}\right) \quad (9)$$

$$v_i(x) = \frac{1}{(\exp(x) + 1)} \quad (10)$$

$$x_i = \sum \alpha_i \bullet \omega_i \quad (11)$$

The adjustment of weight is mainly reflected in the backpropagation of the error, where the square error $E = (1/2)e_i^2$ is propagated as a regulatory signal. The gradient of the modifier is

$$\frac{\partial E}{\partial \omega_i} = \frac{\partial E}{\partial e_i}\frac{\partial e_i}{\partial y_i}\frac{\partial y_i}{\partial x_i}\frac{\partial x_i}{\partial \omega_i} = -e_i v_i'\left(\sum \alpha_i \bullet \omega_i\right)\alpha_i \quad (12)$$

The correction value of the weight is $\triangle\omega_i = -\eta(\partial E/\partial\omega_i)$, where η is the learning rate. A new weight $\omega_i^{(1)} = \triangle\omega_i + \omega_i$ is obtained and substituted back into the above formula to conduct an iterative operation. Weight adjustment is complete when the square error is within the range of tolerance.

4.2. Determining the Model. The sensor is primarily composed of a strain gauge and a measuring circuit. The fault model is established by analyzing the structure of the weighing sensor and fault sampling and by considering the influence of the external environment on the sensor, as shown in Figure 8 in Appendix. See Appendix for fault events corresponding to each place.

As the scale of the model is large, writing the input and output matrices is cumbersome. To show the reasoning and calculation process, the "bridge circuit fault" is used as an example in this study to illustrate faults in the resistance strain weighing sensor, and its FPN fault model is shown in Figure 2. The remaining part of the reasoning process is the same as the example.

4.3. Original Data. According to the method mentioned in Section 4, the vector form of the confidence coefficient of the underlying place was obtained as follows: $\alpha_0 = (0.89, 0.87, 0.84, 0.71, 0.88, 0.93, 0.89, 0.8, 0.87, 0, 0, 0.69, 0, 0.88, 0.9, 0, 0, 0, 0)^T$.

Taking transition T_5, T_7 as an example, the weights of P_4, P_5, P_6, P_7, and P_8 are adjusted using the method described in Section 4. Hypothesis: $\omega_{45} = 0.3$, $\omega_{55} = 0.4$, $\omega_{65} = 0.3$, $\omega_{77} = 0.33$, $\omega_{87} = 0.65$. From statistical calculations, the expectation $\alpha(P_{30}) = 0.6937$, $\alpha(P_{32}) = 0.7003$, $\eta = 0.1$, the largest number of learning steps was set to 4,000, and the square error was 0.1×10^{-5}. The training results are shown in Figures 3 and 4.

The square error after 3928 steps of iterative operation was within the allowable range. The weights of P_4, P_5, P_6, P_7, and P_8 obtained at this point were 0.3936, 0.5160, 0.0904, 0.5177, and 0.4823, respectively. Weight matrix is used to calculate the confidence of the entire Petri net:

$$\omega = \begin{bmatrix}
1 & 0 & 0 & 0 & 0 & 0 & 0 & 0 & 0 & 0 & 0 & 0 & 0 & 0 & 0 & 0 & 0 \\
0 & 1 & 0 & 0 & 0 & 0 & 0 & 0 & 0 & 0 & 0 & 0 & 0 & 0 & 0 & 0 & 0 \\
0 & 0 & 1 & 0 & 0 & 0 & 0 & 0 & 0 & 0 & 0 & 0 & 0 & 0 & 0 & 0 & 0 \\
0 & 0 & 0 & 1 & 0 & 0 & 0 & 0 & 0 & 0 & 0 & 0 & 0 & 0 & 0 & 0 & 0 \\
0 & 0 & 0 & 0 & 0.39 & 0 & 0 & 0 & 0 & 0 & 0 & 0 & 0 & 0 & 0 & 0 & 0 \\
0 & 0 & 0 & 0 & 0.52 & 0 & 0 & 0 & 0 & 0 & 0 & 0 & 0 & 0 & 0 & 0 & 0 \\
0 & 0 & 0 & 0 & 0.09 & 1 & 0 & 0 & 0 & 0 & 0 & 0 & 0 & 0 & 0 & 0 & 0 \\
0 & 0 & 0 & 0 & 0 & 0 & 0.52 & 0 & 0 & 0 & 0 & 0 & 0 & 0 & 0 & 0 & 0 \\
0 & 0 & 0 & 0 & 0 & 0 & 0.48 & 0.42 & 0 & 0 & 0 & 0 & 0 & 0 & 0 & 0 & 0 \\
0 & 0 & 0 & 0 & 0 & 0 & 0 & 0.58 & 0 & 0 & 0 & 0 & 0 & 0 & 0 & 0 & 0 \\
0 & 0 & 0 & 0 & 0 & 0 & 0 & 0 & 1 & 0 & 0 & 0 & 0 & 0 & 0 & 0 & 0 \\
0 & 0 & 0 & 0 & 0 & 0 & 0 & 0 & 0 & 1 & 0 & 0 & 0 & 0 & 0 & 0 & 0 \\
0 & 0 & 0 & 0 & 0 & 0 & 0 & 0 & 0 & 0 & 1 & 0 & 0 & 0 & 0 & 0 & 0 \\
0 & 0 & 0 & 0 & 0 & 0 & 0 & 0 & 0 & 0 & 0 & 1 & 0 & 0 & 0 & 0 & 0 \\
0 & 0 & 0 & 0 & 0 & 0 & 0 & 0 & 0 & 0 & 0 & 0 & 1 & 0 & 0 & 0 & 0 \\
0 & 0 & 0 & 0 & 0 & 0 & 0 & 0 & 0 & 0 & 0 & 0 & 0 & 1 & 0 & 0 & 0 \\
0 & 0 & 0 & 0 & 0 & 0 & 0 & 0 & 0 & 0 & 0 & 0 & 0 & 0 & 1 & 0 & 0 \\
0 & 0 & 0 & 0 & 0 & 0 & 0 & 0 & 0 & 0 & 0 & 0 & 0 & 0 & 0 & 1 & 0 \\
0 & 0 & 0 & 0 & 0 & 0 & 0 & 0 & 0 & 0 & 0 & 0 & 0 & 0 & 0 & 0 & 0
\end{bmatrix} \tag{13}$$

According to the results of the calculation and an analysis of this model, the threshold value of all transitions was set to 0.5.

α_0, W, O, and I were substituted into (1). The reasoning was not concluded until $\alpha_4 = \alpha_3$, $\alpha_3 = (0.89, 0.87, 0.84, 0.71, 0.88, 0.93, 0.89, 0.8, 0.87, 0.7089, 0.72, 0.69, 0.7, 0.88, 0.9, 0.84, 0.67, 0.71, 0.71)^{\mathrm{T}}$. Thereafter, the confidence coefficients of each place were obtained and used as the basis for the forward and backward reasoning.

4.4. Forward and Backward Reasoning

4.4.1. Forward Reasoning. The sensor ran normally and no fault occurred, but symptoms of fault were detected, including "excessively high supply voltage," "broken output lead," "insufficient soldering of cable," "humid environment," and "broken gate of the output adjusting resistance." The initial labeling vector obtained was $K_0 = (1, 0, 0, 1, 1, 0, 0, 0, 1, 0, 0, 0, 0, 0, 1, 0, 0, 0, 0)^T$, and α_3 was substituted into (2) and (3) to calculate the potential transition-enabled matrix $y = (1, 1, 1, 1, 1, 1, 1, 1, 1, 1, 1, 1, 1, 1, 1, 1, 1)^{\mathrm{T}}$. K_0 and y were substituted into (4) to conduct the reasoning calculation. The final results gained were $K_3 = (1, 0, 0, 1, 1, 0, 0, 0, 1, 1, 1, 0, 0, 0, 1, 1, 1, 1, 1)^T$, and $Y_3 = Y_4$. The reasoning was concluded, $Y_3 = (0, 0, 0, 0, 0, 0, 0, 0, 0, 0, 0, 0, 0, 0, 0, 0, 1)^{\mathrm{T}}$, the final labeling vector was K_3, and the fault transmission path is shown in Figure 5. The foregoing conclusions can be used as the basis for fault checking and maintenance to improve the operational stability of the sensor.

4.4.2. Backward Reasoning. Backward reasoning was carried out using the example of "no signal output or small signal output after loading." The initial labeling vector $K_0^- = (0, 0, 0, 0, 0, 0, 0, 0, 0, 0, 0, 0, 0, 0, 0, 0, 1, 0, 0)^{\mathrm{T}}$, and the potential transition-enabled matrix obtained by the forward reasoning $y^- = (1, 1, 1, 1, 1, 1, 1, 1, 1, 1, 1, 1, 1, 1, 1, 1, 1)^{\mathrm{T}}$.

$K_0^-, y^-, I^-, 0^-$ were substituted into (6). As indicated by the reasoning calculation, when $y_3^- = y_2^-$, the reasoning was concluded, and the labeling vector and backward transition matrix were obtained: $K_2^- = (1, 1, 1, 1, 1, 1, 1, 0, 0, 1, 1, 1, 1, 0, 0, 0, 1, 0, 1)^{\mathrm{T}}$ and $y_2^- = (1, 1, 1, 1, 1, 1, 1, 0, 0, 0, 0, 0, 0, 0, 0, 0, 0)^{\mathrm{T}}$. The distribution of places is shown in Figure 6.

As shown in Figure 6, the minimum cut set enabling P_{49} was $G_1 = \{p_1\}$, $G_2 = \{p_2\}$, $G_3 = \{p_3\}$, $G_4 = \{p_4\}$, $G_5 = \{p_4 \bullet p_5\}$, $G_6 = \{p_5\}$, $G_7 = \{p_5 \bullet p_6\}$, $G_8 = \{p_4 \bullet p_5 \bullet p_6\}$, and $G_9 = \{p_7\}$. According to (6), *$f(G_1) = 0.89$, $f(G_2) = 0.87$, $f(G_3) = 0.84$, $f(G_4) = 0.88$, $f(G_5) = 0.795$, $f(G_6) = 0.71$, $f(G_7) = 0.93$, and $f(G_8) = 0.89$*. The fault occurrence probability is shown in Figure 7.

As indicated by Figure 7, the order of diagnosis should be G_7, G_1, G_9, G_6, G_2, G_3, G_5, and G_4. Thus, the speed of diagnosis can be improved.

5. Statistics and Verification of Fault Reasoning

5.1. Fault Statistics. In this study, the maintenance record of CSY-3000 (an instrument manufactured by Zhejiang Golink

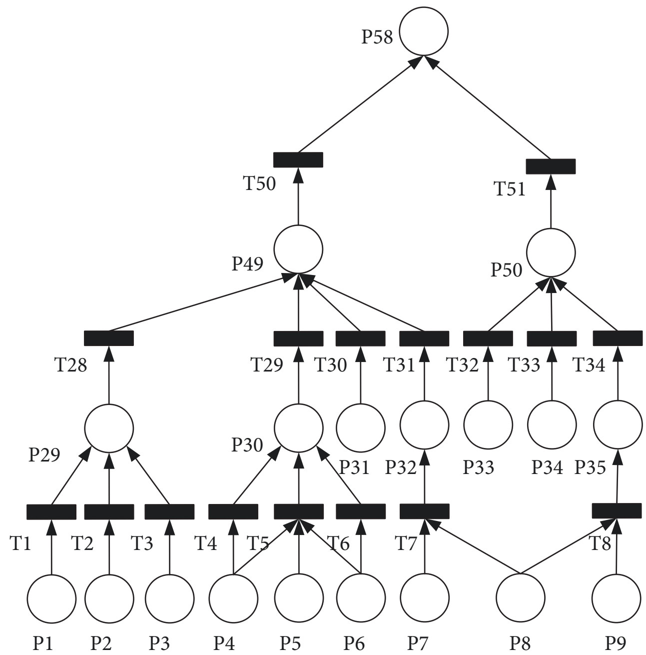

Figure 2: Part of the FPN model.

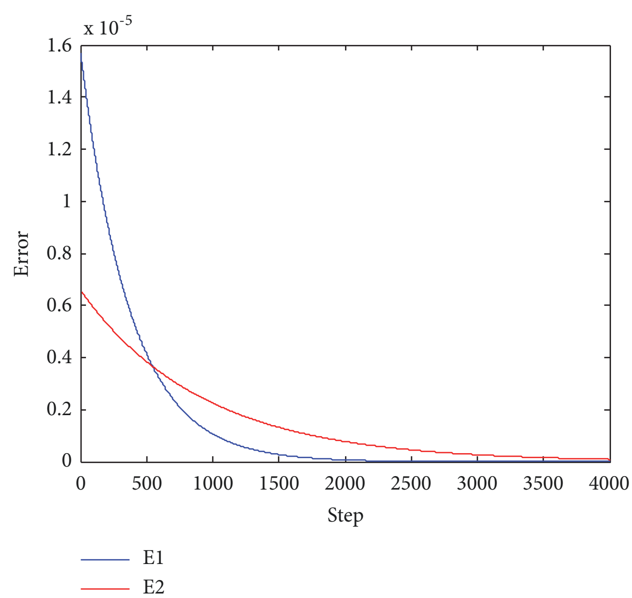

Figure 3: Adjustment curve of square error E.

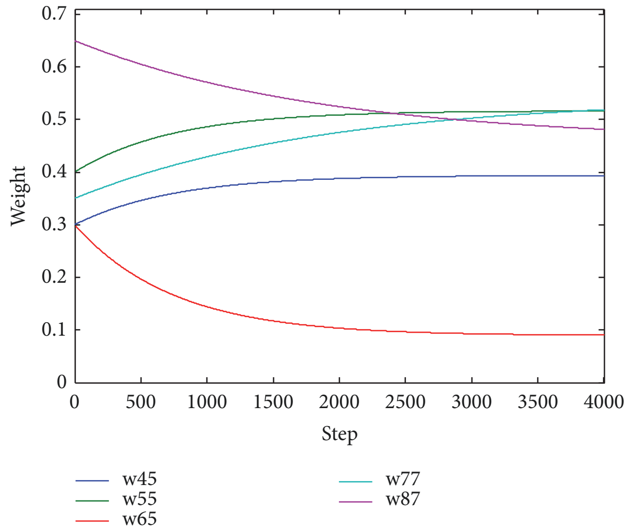

Figure 4: Weighing adjustment curve.

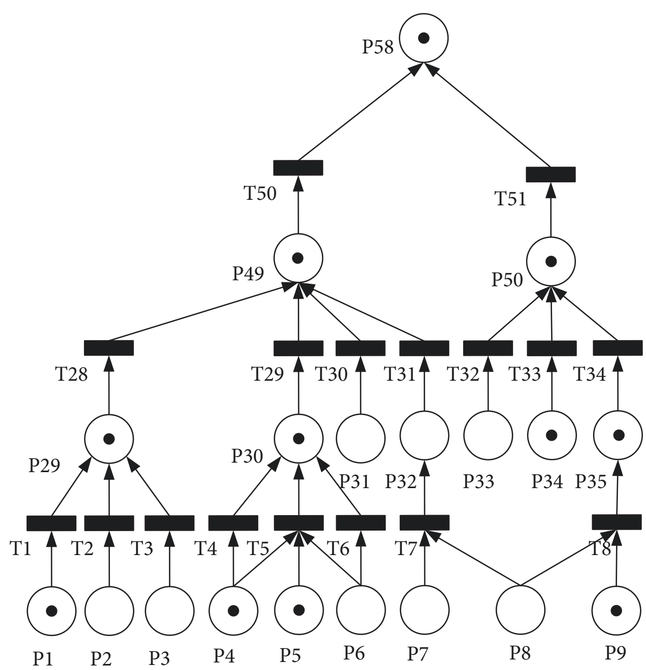

Figure 5: Token distribution after forward reasoning.

Technology Development Co., Ltd., China) for the last two years (2016–2017) and data from the manufacturer's reliability manual ("other" fault causes were introduced due to loss of data records; we render the data true and reliable, including the statistics) were statistically analyzed and compared with the results of reasoning. The data on "no signal output or small signal output after loading" were sorted out, as shown in Table 1.

The correlation coefficient can be obtained based on the data mentioned in Table 1, which can then be used to verify the correctness of the results of reasoning. The correlation coefficient is calculated as follows:

$$r = \frac{\sum_{i=1}^{n}\left(x_i - \overline{x}\right)\left(y_i - \overline{y}\right)}{\sqrt{\sum_{i=1}^{n}\left(x_i - \overline{x}\right)^2 \bullet \sum_{n=1}^{i}\left(y_i - \overline{y}\right)^2}} \quad (14)$$

The average values were calculated first: $\overline{x}=43.4$ and $\overline{y} = 0.74766$. x_i and $y_i$were substituted into (14) to obtain the correlation coefficient $r = 0.8865$. As indicated by the

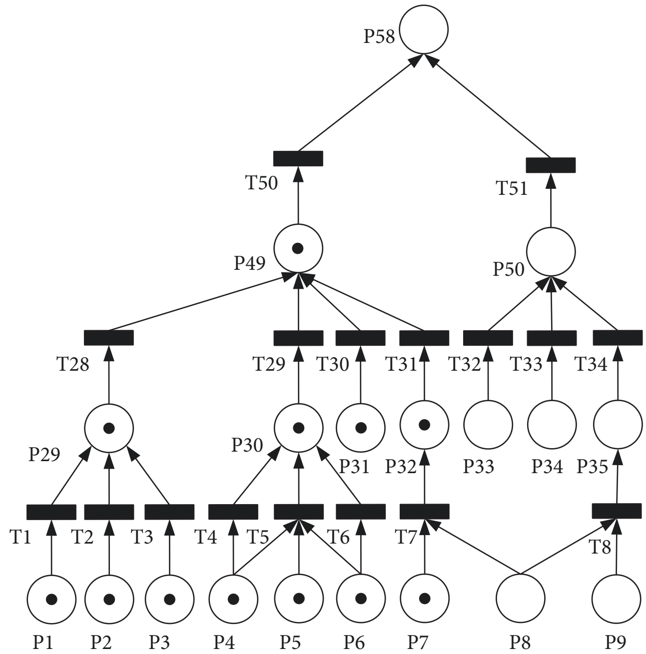

Figure 6: Token distribution after backward reasoning.

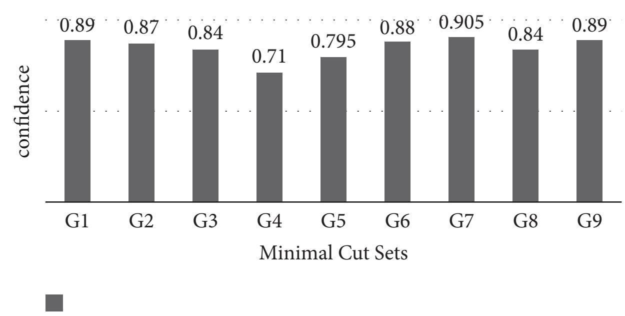

Figure 7: Fault occurrence probability of the minimum cut set.

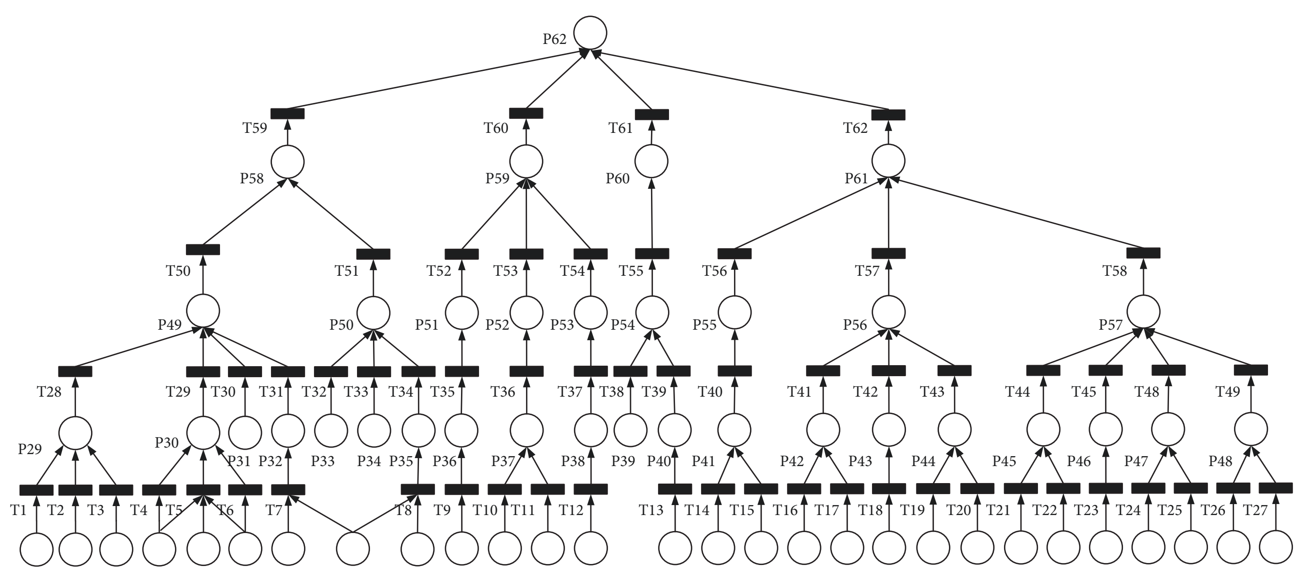

Figure 8: FFPN model diagram of the sensor fault system.

Table 1: Fault-related data.

Causes of fault	Number of faults/frequency (x_i)	Confidence of place (y_i)
P_1	60	0.89
P_2	46	0.87
P_3	40	0.84
P_4	47	0.88
P_5	70	0.93
P_6	58	0.89
P_{29}	34	0.7089
P_{30}	32	0.72
Others	4	0

Table 2: Comparison and validation of different methods.

Reference	[18]		[13]		This study	
Source of weight	None		BP algorithm		BP algorithm	
Confidence of transition	None		Experts' experience		Sigmoid function	
Reasoning method	Data integration		Calculation and reasoning		The modified reasoning method	
Case #	Case 1	Case 2	Case 1	Case 2	Case 1, Case 2	
Field fault	p_1, p_4, p_5	p_9	p_1, p_4, p_5	p_9	p_1, p_4, p_5	p_9
Diagnosis results	p_1, p_4	p_9	p_1, p_4, p_5	p_9	p_1, p_4, p_5	p_9
Undetected	p_5		None		None	
Correlation			0.7516		0.8865	

results of the calculation, those of the diagnosis were strongly correlated with actual statistics.

5.2. Case Analysis. To further verify the accuracy of this method, the techniques proposed in [13, 18] were used to analyze two cases: "no signal output or small signal output after loading" and "unstable indicating instrument." The results are shown in Table 2.

It can be seen from the table that, in terms of effectiveness, compared with the results of [13], the results were verified as valid. From the aspect of fault tolerance, the authors of [13] and this paper observed no leakage detection, whereas the work in [18] reported leakage in "insufficient soldering of cable." In terms of data selection, the other methods were excessively dependent on expert experience, whereas this paper used a neural network and the sigmoid function as trigger modes, thus increasing the value of the correlation coefficient in the final diagnosis and bringing it closer to the actual fault state.

6. Conclusion

A method of fault diagnosis in Petri net sensors was proposed in this study based on a new confidence reasoning method and was applied to the fault prediction and diagnosis of a resistance strain weighing sensor.

(1) A fault diagnosis model of the resistance strain weighing sensor was established based on the structure, operating characteristics, and fault occurrence of the sensor.

(2) A neural network algorithm was applied to determine the parameters of the model, and a confidence reasoning formula proposed to deduce the pathway and mode of fault propagation, which improved speed and diagnosis efficiency.

(3) Forward and backward reasoning were combined to obtain the order of occurrence of faults for each component, which helps avoid blind detection and maintenance. The relationship between events was clearly presented by the Petri net diagrams.

Despite the contributions of this study, the proposed method has some limitations. The logical relationship, the optimization of threshold setting in the sensor model, and the numerical simulation of the model will be studied in future work.

Appendix

See Figure 8 and Table 3.

Data Availability

The data used to support the findings of this study are available from the corresponding author upon request.

Conflicts of Interest

The authors declare that there are no conflicts of interest.

Acknowledgments

The work was supported by the National Natural Science Foundation of China (no. 61503224), Shandong Natural Science Foundation of China (no. ZR2017MF048), Major

Table 3: Petri net library of fault events.

Code	Meaning	Code	Meaning	Code	Meaning
p_1	Excessively high supply voltage	p_{22}	The design of the strain gauge does not accord with Saint Venant's Principle	p_{43}	The maximum stress point lies outside the strain region
p_2	Lightning stroke	p_{23}	Elastic components are affected by contact stress	p_{44}	Inherent linear difference of the hardware
p_3	"Surge voltage" caused by unstable supply voltage	p_{24}	Relatively large shearing strength generated on the surface of elastic components	p_{45}	Uneven strain distribution
p_4	Broken output lead	p_{25}	Poor heat dissipation of the resistance wire after being powered on	p_{46}	Viscous flow of elastic components
p_5	Insufficient soldering of cable	p_{26}	Excessively high temperature	p_{47}	Thermoelastic effect of elastic components
p_6	Disconnected wire	p_{27}	Poor welding quality	p_{48}	Poor contact of the resistance strain gauge
p_7	Excessively large impact during weighing	p_{28}	Aging of the strain adhesive	p_{49}	No signal output or small signal output after loading
p_8	Broken cable	p_{29}	Resistance strain gauge burnout	p_{50}	Unstable indication instrument
p_9	Humid environment	p_{30}	Zero-differential circuit output	p_{51}	Slow decline in insulation resistance value
p_{10}	The charged nitrogen is not dried	p_{31}	Incorrect direction of adherence of the resistance strain gauge	p_{52}	Deformation or damage to the seal membrane
p_{11}	Overloaded weighing	p_{32}	Broken bridge resistance or compensating resistance	p_{53}	Unstable compensating resistance
p_{12}	Loading impact	p_{33}	Damaged circuit insulation	p_{54}	Overheated grid
p_{13}	Excessively long compensating resistance wire	p_{34}	Broken gate of the output-adjusting resistance	p_{55}	Hysteresis error
p_{14}	Air bubble resistance caused by the adherence of strain gauge	p_{35}	Output with interference signal	p_{56}	Excessively large non-linear deviation
p_{15}	Irrational design of contact between elastic components and the pushing felt	p_{36}	Protective agent affected by dampness	p_{57}	Relatively large creep error
p_{16}	Excessively large friction coefficient of the cushion	p_{37}	Plastic deformation of the strain gauge	p_{58}	Bridge circuit fault
p_{17}	Aging of the welding process of the strain gauge	p_{38}	deformation of the compensating consistency	p_{59}	Unstable zero output

Table 3: Continued.

Code	Meaning	Code	Meaning	Code	Meaning
p_{18}	Reduced sensitivity of the strain gauge	p_{39}	No aging treatment of the compensating consistency wire	p_{60}	Excessively large drifting of zero temperature
p_{19}	Irrational design of elastic components	p_{40}	"Hot spot effect"	p_{61}	Excessively large measuring error
p_{20}	Irrational design of flexible isolation	p_{41}	Recovery of deformation of the retardant elastic components	p_{62}	Weighing sensor fault
p_{21}	Serious aging of the grip zone	p_{942}	Excessively large sensitivity of diaphragm shunting		

Research Development Program of Shandong Province of China (no. 2016GSF117009), Qingdao Minsheng Science and Technology Plan Project (no. 17-3-3-88-nsh), and Shandong University of Science and Technology Postgraduate Innovation Program (SDKDYC180232).

References

[1] L. Niu, F. Ren, M. Zhang, and Q. Bai, "A Concurrent Multiple Negotiation Protocol Based on Colored Petri Nets," *IEEE Transactions on Cybernetics*, vol. 47, no. 11, pp. 3692–3705, 2017.

[2] M. Gao, M. Zhou, X. Huang, and Z. Wu, "Fuzzy reasoning Petri nets," *IEEE Transactions on Systems, Man, and Cybernetics - Part A: Systems and Humans*, vol. 33, pp. 314–324, May 2003.

[3] J. Sun, S.-Y. Qin, and Y.-H. Song, "Fault diagnosis of electric power systems based on fuzzy Petri nets," *IEEE Transactions on Power Systems*, vol. 19, no. 4, pp. 2053–2059, 2004.

[4] X. Luo and M. Kezunovic, "Implementing fuzzy reasoning Petri-nets for fault section estimation," *IEEE Transactions on Power Delivery*, vol. 23, no. 2, pp. 676–685, 2008.

[5] L. Wang et al., "Knowledge representation and general Petri net models for power grid fault diagnosis," *IET Generation, Transmission & Distribution*, vol. 6, no. 9, pp. 866–873, 2015.

[6] H. Yuan, H. Yuan, and X. Li, "Fuzzy petri nets reasoning for application of electric control system fault diagnosis," in *Proceedings of the 2006 IEEE Conference on Robotics, Automation and Mechatronics*, Thailand, June 2006.

[7] J. Jung, C.-C. Liu, M. Hong, M. Gallanti, and G. Tornielli, "Multiple hypotheses and their credibility in on-line fault diagnosis," *IEEE Transactions on Power Delivery*, vol. 16, no. 2, pp. 225–230, 2001.

[8] L. Wei, W. Guo, F. Wen, G. Ledwich, Z. Liao, and J. Xin, "An online intelligent alarm-processing system for digital substations," *IEEE Transactions on Power Delivery*, vol. 26, no. 3, pp. 1615–1624, 2011.

[9] C. J. Edwards, E. M. Davidson, S. D. J. McArthur, I. Watt, and T. Cumming, "Flexible model-based alarm processing for protection performance assessment and incident identification," *IEEE Transactions on Power Systems*, vol. 28, no. 3, pp. 2584–2591, 2013.

[10] Y. N. Wang, J. F. Ye, G. J. Xu, Q. M. Chen, H. Y. Li, and X. R. Liu, "Novel hierarchical fault diagnosis approach for smart power grid with information fusion of multi-data resources based on fuzzy petri net," in *Proceedings of the 2014 IEEE International Conference on Fuzzy Systems (FUZZ-IEEE '14)*, pp. 1183–1189, July 2014.

[11] Y. Zhang, F. Wen, C. Chung et al., "A fuzzy Petri net based approach for fault diagnosis in power systems considering temporal constraints," *International Journal of Electrical Power & Energy Systems*, vol. 78, pp. 215–224, 2016.

[12] M. T. Xin and S. Z. Shi, "Metal model based fuzzy Petri nets back propagation learning algorithm," in *Proceedings of the IMACS Multiconference on "Computational Engineering in Systems Applications", CESA*, pp. 1853–1857, China, October 2006.

[13] S. Wen, J. Ye, and Z. Zhu, "A feedback adaptive fuzzy Petri net model for context reasoning," in *Proceedings of the 5th International Conference on Pervasive Computing and Applications, ICPCA10*, pp. 313–319, Slovenia, December 2010.

[14] P. M. Bao, "Learning capability in fuzzy Petri nets based on BP net," *Chinese Journal of Computers. Jisuanji Xuebao*, vol. 27, no. 5, pp. 695–702, 2004.

[15] R. P. Brent, "Fast Training Algorithms for Multilayer Neural Nets," *IEEE Transactions on Neural Networks and Learning Systems*, vol. 2, no. 3, pp. 346–354, 1991.

[16] X. Li, W. Yu, and F. Lara-Rosano, "Dynamic knowledge inference and learning under adaptive fuzzy Petri net framework," *IEEE Transactions on Systems, Man, and Cybernetics, Part C: Applications and Reviews*, vol. 30, no. 4, pp. 442–450, 2000.

[17] X. Wang, C. Mahulea, and M. Silva, "Diagnosis of time Petri nets using fault diagnosis graph," *Institute of Electrical and Electronics Engineers Transactions on Automatic Control*, vol. 60, no. 9, pp. 2321–2335, 2015.

[18] J. Zhang, J. Cao, and F. Gao, "Multivariable dynamic system fault diagnosis using nonlinear spectrum and SVM fusion," in *Proceedings of the 2015 IEEE International Conference on Computational Intelligence and Virtual Environments for Measurement Systems and Applications, CIVEMSA 2015*, China, June 2015.

[19] F. Sun, Y. Cheng, C. Cheng, and X. Bian, "Intelligent evaluation of fault status in power transformer based on fuzzy fault Petri net," in *Proceedings of the 35th IEEE Electrical Insulation Conference, EIC 2017*, pp. 104–107, USA, June 2017.

[20] Y. Wang and D. Qiu, "A method of synthetical fault diagnosis for power system based on fuzzy hierarchical Petri net," in *Proceedings of the 13th IEEE International Conference on Mechatronics and Automation, IEEE ICMA 2016*, pp. 254–258, China, August 2016.

[21] S.-M. Chen, J.-S. Ke, and J.-F. Chang, "Knowledge representation using fuzzy Petri nets," *IEEE Transactions on Knowledge and Data Engineering*, vol. 2, no. 3, pp. 311–319, 1990.

[22] Y. Liang and B. Yuan, "Method for generating fuzzy Petri nets fault diagnosis model based on rough set theory," in *Proceedings of the 2010 2nd International Conference on Future Computer and Communication*, pp. V1-411–V1-414, Wuhan, China, May 2010.

[23] J. P. Wilkinson, "Nonlinear resonant circuit devices (Patent style)," *U.S. Patent*, vol. 3, pp. 624-12, 1990.

[24] F. Zhou, R. J. Jiao, Q. Xu, and K. Takahashi, "User Experience Modeling and Simulation for Product Ecosystem Design Based on Fuzzy Reasoning Petri Nets," *IEEE Transactions on Systems, Man, and Cybernetics - Part A: Systems and Humans*, vol. 42, pp. 201–212, 2012.


Advances in Operations Research
Advances in Decision Sciences
Journal of Applied Mathematics
The Scientific World Journal
Journal of Probability and Statistics
International Journal of Mathematics and Mathematical Sciences
Hindawi
Submit your manuscripts at
www.hindawi.com
Journal of Optimization
International Journal of Engineering Mathematics
International Journal of Analysis
Journal of Complex Analysis
Advances in Numerical Analysis
Mathematical Problems in Engineering
International Journal of Differential Equations
Discrete Dynamics in Nature and Society
International Journal of Stochastic Analysis
Journal of Mathematics
Journal of Function Spaces
Abstract and Applied Analysis
Advances in Mathematical Physics